

FOOTING WITH INVERTED PYRAMIDAL PROTRUSIONS FOR SETTLEMENT CONTROL IN SANDY DEPOSITS

*Chee-Ming Chan and Muhammad Arif Amzar Mohd. Yusuf

Faculty of Engineering Technology, Universiti Tun Hussein Onn Malaysia, Malaysia

*Corresponding author, Received: 20 Nov. 2016, Revised: 20 Feb. 2017, Accepted: 10 March 2017

ABSTRACT: This paper examines the feasibility of using an innovative footing with a corrugated base to enhance the load-bearing capacity of shallow foundation, and to reduce the substructure's subsidence as a whole or differentially. The corrugated base consists of inverted pyramidal protrusions which give a 3-fold advantages: (1) the pointed tips help smoothen the process of installation on site, (2) the protrusions provide additional contact surface between the foundation and the soil for better load-bearing, (3) the corrugated base entraps soil between the individual protrusions, improving the foundation's stability against settlement and sliding. Scaled models of the 8 cm x 8 cm footing were produced using 3D printing: CONTROL- smooth base, Design A corrugated base with 16 inverted pyramidal protrusions of 2 cm x 2 cm x 2 cm each, and Design B-corrugated base with 64 inverted pyramidal protrusions of 1 cm x 1 cm x 1 cm each. Both designs had the same contact surface area with the soil, though the penetration depth of the pyramids and the space between the protrusions varied. Maintained load tests were carried out in simulated soil beds to determine the improved performance of the foundation. It was shown that the corrugated slabs reduced settlement up to over 85 % compared with the conventional smooth-base footing, with Design B giving slightly better results. It was also observed that the larger pyramidal protrusions (Design A) tended to entrap air between them, forming air cushions which resisted further penetration of the corrugated base into the soil, i.e. inhibiting mobilization of the maximum load-bearing capacity.

Keywords: Shallow foundation, Settlement, Load-bearing, Contact surface, Friction, Sliding, Roughened base

1. INTRODUCTION

A shallow foundation is defined as a substructure with the primary function of transferring imposed loads from the superstructure to the underlying stratum safely. The embedded depth of the foundation could range between 3 to 5 times its width [1-3], but the embedded depth-to-breadth (D_f/B) ratio is generally kept below 5 [4]. Note however that historically Terzaghi (1943) expounded the ratio to be no more than 1 indeed [5]. Considering that a shallow foundation would transfer loads to relatively shallow depths, the soil stratum lying immediately below the ground surface plays an important role in the substructure-soil interaction, i.e. the effectiveness of load-bearing and resulting settlement control.

Underlying sand layer is also known to be susceptible to liquefaction and to undergo large deformations due to earthquake loading [6-8]. In addition, rapid alternation of the dynamic load vector in an earthquake event, i.e. amplitude and direction, could cause instantaneous changes of the shear strength mobilized within the sand supporting the foundation, leading to gradual subsidence failures rather than sudden bearing capacity collapse [9]. Loss of soil-foundation contact is the main factor contributing to the accumulated plastic displacement of the footing, which causes progressive degradation of the bearing capacity [10-

12]. In cases like these, stability of the shallow foundation could be enhanced with strengthened interface between soil-footing to minimize the loss of contact area.

Past work on the performance of shallow foundation with laboratory scale simulations are not unknown of. Boiko & Alhassan et al. [13], for instance, examined the load-bearing behaviour of wedge-shape footings embedded in sand and found the bearing capacity to be more superior to that of a squarish or T-shape footing. The improvement was attributed to the surcharge effect provided by the soil mass above the base of the tapered wedge, countering heaving of the active zones beneath the foundation. Footings with short open- and close-end stumps were experimented by Chan [14] for settlement reduction in soft clay soils as an economical solution to excessive and non-uniform subsidence problems in waterlogged, low-lying areas. Also, Vanapalli & Mohamed [15] and Al-Khuzaei [16] studied the scale effects of shallow foundation in sand with relation to bearing capacity, while Sitharam & Sireesh [17] and Moghaddas & Dawson [18] investigated shallow foundations seated on sand layer reinforced with geosynthetics, such as geogrid, geocell and geotextile. Besides, Makarchian & Badakhshan [19] tested circular and square footings with 0.33 cm thick geogrid attached to the base and reported more significant bearing capacity improvement and settlement control for

the former in a geogrid-reinforced sand bed. No observation was made of the effect of the geogrid base on the overall performance of the footings though.

In the present study, an innovative slab with corrugated base was designed and examined for its expediency as a shallow foundation in sand. 8 cm x 8cm square footings were produced from Acrylonitrile Butadiene Styrene (ABS) plastic using a 3D printer for tests in model sand beds. The footings included a smooth base CONTROL, Design A and Design B with 16 and 64 protrusions of inverted pyramids respectively to form a corrugated base. Maintained load tests were carried out to examine the performance of the scaled slabs with corrugated bases in settlement reduction, via both enhanced soil-foundation interaction and more effective load distribution mechanism.

2. MATERIALS AND METHODS

2.1 Model soil bed

The Acrylic model box measured 90 mm x 90 mm and 150 mm, where the soil bed was formed up to 80 mm height from the base of the box (Fig. 1). The soil bed consisted of carefully lain layers of materials (from top to bottom): 10 mm of fine sand (0.063-0.2 mm) for placement of the slab, 30 mm of medium sand (0.2-0.63 mm), 10 mm of kaolin at slightly above the plastic limit to simulate a sandwiched soft clay layer, followed by 30 mm of medium sand. The sand were deposited in layers using a funnel to ensure uniformity.

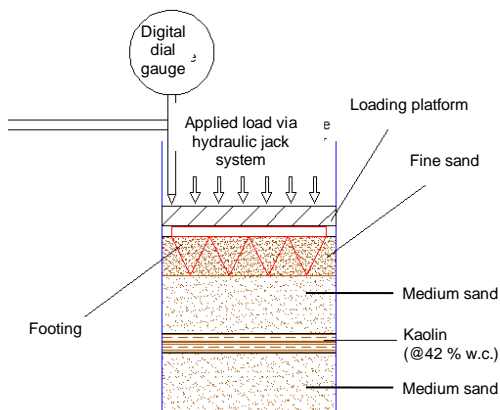


Fig. 1 Model test setup.

2.2 Footings

3 model footings were prepared from ABS for the purpose of the present study (Fig. 2). All the footings had a plan area of 8 cm x 8 cm and 0.7 cm thickness. The CONTROL footing had a smooth base and measured as above. 2 slabs with corrugated base were designed and fabricated, namely Design A and Design B. Design A had 16

inverted pyramidal protrusions at the base, each measuring 2 cm x 2 cm x 2 cm, while Design B had 64 inverted pyramidal protrusions of 1 cm x 1 cm x 1 cm each. Although both designs had different numbers of protrusions, they shared the same contact surface area with the soil, i.e. 143.10 cm², compared to 64 cm² for the CONTROL slab. This gave a difference of 123 % between the total contact surface area available for the smooth and corrugated bases. Total volume of the inverted pyramids was 87.47 cm³ and 63.13 cm³ for Design A and Design B respectively, with a difference of about 30 % between the two.

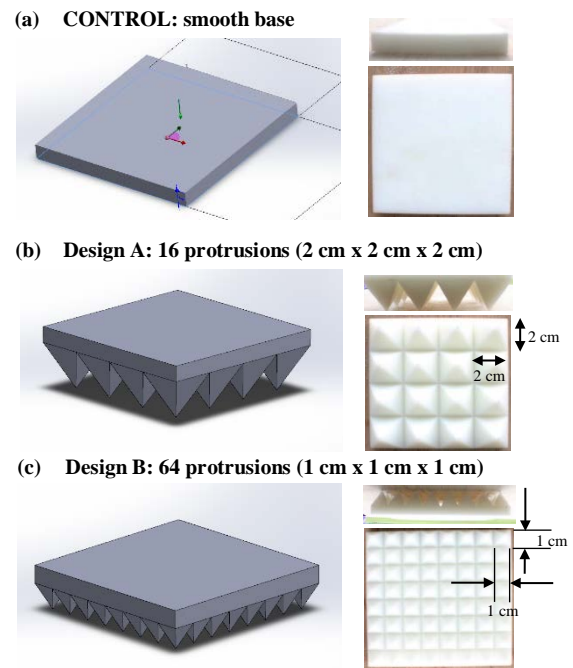


Fig. 2 Model footings of 8 cm x 8 cm.

2.3 Load test

Referring to Fig. 1, compressive load was applied in the tests using the ENERPAC hydraulic jack system, where the loading piston transferred the load to the foundation via a plywood platform atop the footing. The vertical displacement was read off a digital dial gauge in contact with the loading platform. A vertical stress of 500 kPa was applied throughout each test while the settlement was recorded at fixed time intervals of 0, 10, 20, 30, 40, 50 seconds, followed by 1, 2, 4, 6, 8 10 minutes till constant reading of the dial gauge was reached, i.e. imposed stresses distributed into the grounds via the footing and settlement ceased.

3. RESULT ANALYSIS AND DISCUSSIONS

3.1 Load-Settlement relationship

Fig. 3, with the vertical displacement (D) normalised against the maximum settlement recorded for the CONTROL (D_o). Effectiveness of the innovative footings on settlement control was apparent, where Design A and Design B reduced the total settlement by 27 and 59 % respectively compared to CONTROL. The better load-bearing performance of Design B is attributed to the greater number of inverted pyramidal protrusions at the footing's base, i.e. 4 times that of Design A. In fact, Design B outdid Design A by almost 50 % in terms of settlement reduction.

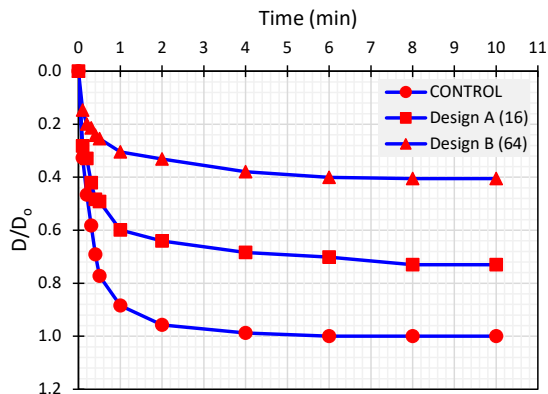


Fig. 3 Normalised settlement vs. time plots.

The load-settlement plots are as compiled in Considering that the total surface area available for full contact with the soil is the same for both designs, despite difference in the number of protrusions, it is postulated that settlement mitigation by the corrugated base was essentially per point and not per area of soil-footing interface. Besides, the seemingly dramatic displacement observed in all footings at initial stage occurred in descending time lapse for CONTROL (0.7 min) > Design A (0.5 min) > Design B (0.3 min). This is suggestive of the corrugated base impeding excessive subsidence of the footing upon loading, consequently minimizing the subsequent settlement as load was gradually transferred to the grounds beneath the footing.

3.2 Settlement rate

The primary and secondary settlement rates were derived from the settlement plots similar to Fig. 3 to illustrate the cessation of subsidence with time. Primary settlement depicts the initial vertical displacement upon loading while secondary settlement represents the gradual transition towards plateau in the load-settlement plots. As shown in Fig. 4, the primary and secondary settlement rates for Design A were 1.7 and 1.2 times respectively that of CONTROL, compared with the corresponding 3.2 and 1.4 times of CONTROL for Design B. Apparently the additional protrusions in Design B was advantageous in prolonging the initial

subsidence time lapse (i.e. $\approx 50\%$ lower settlement rate), hence improving the overall stability of the foundation and structure supported. On the other hand, the secondary settlement for all cases were very much similar, though Design B appeared to take a slightly longer time to undergo the same magnitude of vertical displacement. It follows that the corrugated base with larger contact surface area for both Design A and Design B were more expedient for initial settlement control and reduction. This contrasts with the subsequent secondary settlement which were relatively negligible even for the conventional smooth base footing.

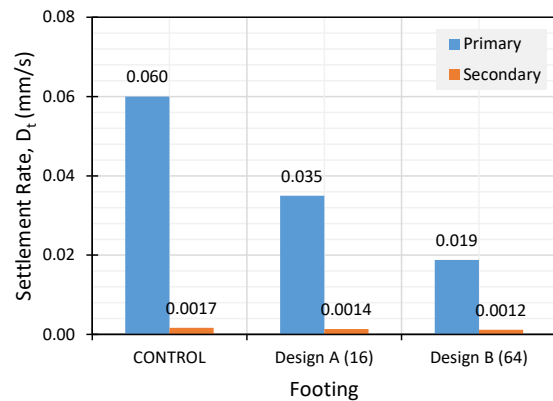


Fig. 4 Primary and secondary settlement rates.

3.3 Contact surface

Fig. 5 summarizes the effect of contact surface area between the footing and soil on the settlement. The bar chart represents the contact surface area (A) and the line plot depicts the final settlement (D_f) recorded for each footing. Significant settlement reduction was observed with the corrugated base which provided 2.3 times more contact surface for soil-footing interaction compared with the CONTROL. This was not unexpected considering the more effective load distribution taking place in the improved base design, i.e. Design B > Design A > CONTROL.

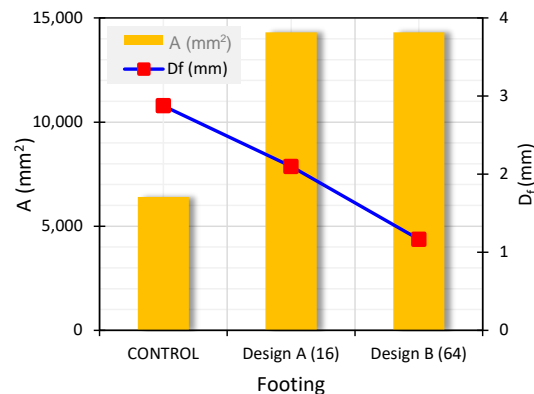


Fig. 5 Effect of contact surface on settlement.

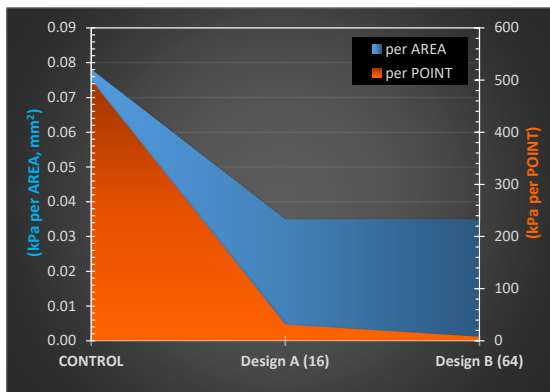
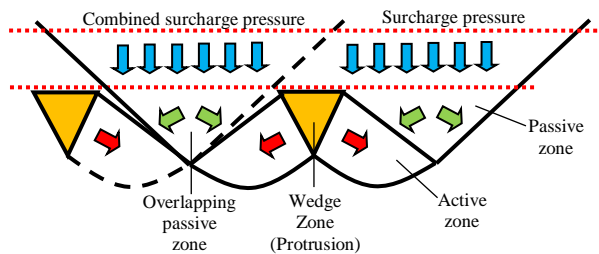


Fig. 6 Stress distribution per contact surface area and protrusion points.



Revisualised Terzaghi's bearing capacity model (with exaggerated inter-protrusion distance).

Fig. 7 Overlapping passive zones resulting in settlement 'lock-in' effect.

It is interesting to note the almost linear settlement reduction recorded for the 3 footings (Fig. 5). However it also highlights the non-correlation between the contact surface area and subsidence control. This is evident from the $\approx 45\%$ difference in settlement recorded, notwithstanding the same surface area for both Design A and Design B. Examining the stress distribution per point of protrusion (Fig. 6), each pyramidal protrusion in Design B transmitted 75% less stress than their counterparts in Design A. In a similar comparison, the stress sustained by the single contact surface of CONTROL was 94-95% greater than each point in the slabs with corrugated base.

This could explain the remarkable settlement reduction recorded for the new footings, where the imposed load was apportioned into the underlying grounds via the individual protrusion. Another factor contributing to the improved load transfer mechanism could be the firmer interface between the footing's base and the underlying soil. This could be illustrated with Terzaghi's classic bearing capacity model for shallow foundation with some minor modifications (Fig. 7). Each pyramidal protrusion with the pointed tip would penetrate the soil and wedge in to form individual active-passive zonation of the load-bearing system. The

overlapping passive zones of adjacent wedge-like protrusion, combined with the shared overlying surcharge pressure would effectively counter the downward displacement of the footing under load. In effect, the neighbouring passive zones coinciding with each other create a resultant force on the respective active zones of the protrusions against further settlement. This 'locking' effect would understandably diminish with increased distance between the protrusions due to detachment of the overlapped passive zones.

3.4 Air cushion effect

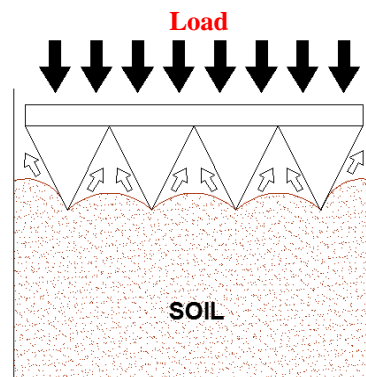


Fig. 8 Formation of air cushion between the protrusions.

In conjunction with the postulation above using the adapted Terzaghi's bearing capacity model in Fig. 7, another phenomenon observed in the load test of the footings with corrugated base was the air cushion effect. As presented in Fig. 8, penetration of the corrugated footing into the sand layer may be partially impeded by entrapped air between the protrusions. Apart from the protrusions along the boundary of the slab, it would seem inevitable that the intermediate inverted pyramids would entrap air released from the sand as the footing was installed in the soil layer.

The entrapped air buffer could prevent further downward displacement of the footing even with continuous loading. On one hand, this occurrence could contribute to overall settlement reduction via additional resistance against the load applied. On the other hand, the air cushion could also adversely prevent full utilization of the contact surface between the protrusions and the soil, resulting in under-mobilised point-based as well as area-based load distribution. Whether or not the opposing effects of the air buffer cancel out one another or that one overshadows the other was neither investigated nor proven in the present study. If the negative outweighs the positive, through-holes can be predrilled in the slab to allow escape of the air, eliminating formation of the air cushion.

4. CONCLUSIONS

Overall the footings with corrugated base were found to be effective in settlement control compared to the conventional footing with a smooth base, i.e. CONTROL. The extra protrusions at the base appeared to capture initial settlement upon loading and to keep overall settlement minimal subsequently: Design B with 64 protrusions outperformed Design A (16 protrusions) by almost 50 %, notwithstanding the same contact surface area shared by both footings. The corrugated base was also found to be more effective for initial settlement reduction rate which made up most of the final settlement recorded. The settlement reduction is mainly attributed to more effective point-base load distribution, the overlapping passive zones of neighbouring protrusions, as illustrated in Terzaghi's adapted bearing capacity model for shallow foundation, and the cushion effect of air entrapped between the protrusions.

5. ACKNOWLEDGEMENT

The work presented was partially funded by ORICC, UTHM. Technical support by the university's Geotechnical Lab and RECESS are duly acknowledged too.

6. REFERENCES

- [1] Shakiba rad, S., Heshmati, A. A. & Salehzadeh, H. (2011). Application of Adaptive Neuro-Fuzzy Inference System (ANFIS) to predict the ultimate bearing capacity of shallow foundation on cohesionless soil. *Electronic J. Geotech. Eng.*, 16, Bundle S, 1459-1469.
- [2] Das, B. M. (2010). *Principles of Foundation Engineering*, 7th ed. CL Engineering.
- [3] Das, B. M. (1999). *Shallow Foundations: Bearing Capacity and Settlement*. CRS Press LLC.
- [4] Ministry of Business, Innovation and Employment, NZ. (2012). *Guidance on Detailed Engineering Evaluation of Non-residential Buildings: Pt. 3 Technical guidance, Sec. 5 Foundations*. New Zealand: Engineering Advisory Group, Ministry of Business, Innovation and Employment (EAG-MBIE).
- [5] von Terzaghi, K. (1943). *Theoretical Soil Mechanics*. New York: John Wiley & Sons, Inc.
- [6] Chu, D., Stewart, J. P., Lin, P. S. & Boulanger, R. W. (2006). Cyclic softening of low-plasticity clay and its effect on seismic foundation performance. *Proc. 4th Int. Conf. Earthquake Engineering, Taipei, Paperno.287*.
- [7] Mendoza, M. J. & Auvinet, G. (1998). Behaviour of building foundations in Mexico City. *Earthquake Spectra*, no. 4, pp. 835-853.
- [8] Crespellani, T., Madiati, C. & Vannucchi, G. (1999). Seismic bearing capacity and settlements of shallow foundations. *Proc. 2nd International Symposium Pre-failure Deformation Characteristics of Geomaterials*, Torino, Italy, pp. 625-632.
- [9] Cascone, E. & Casablanca, O. (2016). Static and seismic bearing capacity of shallow strip footings. *Soil Dynamics & Earthquake Eng.*, no. 84, pp. 204-223.
- [10] Shirato, M., Kouno, T., Asai, R., Nakatani, S., Fukui, J. & Paolucci, R. (2008). Large-scale experiments on nonlinear behaviour of shallow foundations subjected to strong earthquakes. *Soils & Found.*, vol. 48, no. 5, pp. 673-692.
- [11] Knappett, J. A., Haigh, S. K. & Madabhushi, S. P. G. (2006). Mechanism of failure for shallow foundations under earthquake loading. *Soil Dynamics & Earthquake Eng.*, vol. 26, no. 12, pp. 91-102.
- [12] Maugeri, M., Musumeci, G., Novità, D. & Taylor, C. A. (2000). Shaking table test of failure of a shallow foundation subjected to an eccentric load. *Soil Dynamics & Earthquake Eng.*, no. 20, pp. 435-444
- [13] Boiko, I. L. & Alhassan, M. (2013). Effect of vertical cross-sectional shape of foundation in settlement and bearing capacity of soils. *Procedia Engineering*, no. 57, pp. 207-212.
- [14] Chan, C-M., Wong, P-Y. & Lee, C-C. (2010). Subsidence control of construction on soft soils with "Akar Foundation". *J. Modern Applied Science*, vol. 4, no. 8, pp. 12-23.
- [15] Vanapalli, S.K. & Mohamed, F.M.O. (2013). Bearing capacity and settlement of footings in unsaturated sands. *Int. J. Geomate*, vol. 5, no. 1, pp. 595-604.
- [16] Al-Khuzaei, H. M. (2011). Verification of scale effect of shallow foundation in determination of bearing capacity of sand. *Al-Rafida in Engineering*, vol. 2, no. 2, pp. 1-11.
- [17] Moghaddas Tafreshi, S. N. & Dawson, A. R. (2010). Comparison of bearing capacity of a strip footing on sand with geocell with planar forms of geotextile reinforcement. *Geotextiles & Geomembranes*, vol. 28, pp. 72-84.
- [18] Sitharam, T.G. & Sireesh, S. (2004). Model studies of embedded circular footing on geogrid-reinforced sand beds. *Ground Improvement*, vol. 8, no. 2, pp. 69-75.